Energy Conversion and Management: X 27 (2025) 101136

Contents lists available at ScienceDirect

Energy Conversion and Management: X

journal homepage: www.sciencedirect.com/journal/energy-conversion-and-management-x

Cost effective hydrogen production of coupled photovoltaic and electrolyzer systems considering plant lifetime and geographical location

D. Vizza [a], R. Caponi [a], E. Bocci [a], L. Del Zotto [b], C. Bassano [c,*]

[a] Department of Engineering Science, Guglielmo Marconi University, Rome, Italy
[b] Università Telematica e-Campus, Novedrate, CO, Italy
[c] ENEA, Italian Agency for New Technologies, Energy and Sustainable Economic Development, Via Anguillarese, 301, 00123 Rome, Italy

ARTICLE INFO

Keywords:
Levelized cost of hydrogen
Electrolyzer control logic
Grid-connected systems
Renewable energy integration
Hydrogen

ABSTRACT

Advancements in electrolysis technologies, coupled with improvements in associated production processes and public incentive programs, are progressively enabling the widespread deployment of megawatt-scale electrolyzers. While these policies are crucial in the short term to support the adoption of emerging technologies and the transformation of industrial processes, substantial focus must be directed toward optimizing technical solutions. This study aims to determine the cost-optimal configuration of a grid-connected system comprising a photovoltaic (PV) production plant and an electrolyzer. This will be accomplished using advanced simulation models that account for the load and thermal cycles, the geographical location of production sites, and the operational lifespan of the installations. The simulation will identify the optimal ratio between the PV array and the electrolyzer to minimize the LCOH (Levelized Cost of Hydrogen). A sensitivity analysis of the PV capacity, considering site-specific irradiation, will be conducted to achieve this objective. The study further delves into the evaluation of the LCOH depending on the utilization of the stacks and alternative management control logic. The findings from the study suggest that the optimal PV:ELE ratio ranges from 1.5:1 to 1.8:1 based on geographical location and highlight an LCOH reduction of about 10 % while coupling the electrolyzer with a PV monoaxial tracking installation over a fixed setup. Ultimately, the analysis of alternative stack usage strategies demonstrates that dynamically balancing stack utilization ensures the lowest LCOH compared to all other tested alternatives.

1. Introduction

Hydrogen and its application have emerged as a prominent focus of energy research over recent decades, driven by growing interest and substantial scientific inquiry. The proliferation of studies within this area is exemplified by a comprehensive analysis which identified 1,275 documents related to the hydrogen economy [1]. Moreover, research specifically dedicated to green hydrogen has shown exponential growth in recent years, rising sharply from approximately 10 studies per year in 2010 to nearly 70 studies annually in 2023 [2].

Such sustained academic attention underscores a broad consensus among researchers, who increasingly recognize hydrogen as a pivotal element of global sustainable energy strategies and an essential factor in achieving a successful energy transition [3]. This recognition stems largely from hydrogen's distinctive capability to provide large-scale, long-term energy storage, thanks to its inherently high energy density and extended lifetime compared to other solutions [4], especially in the case of high market penetration of renewable energy sources [5]. Indeed, hydrogen-based energy storage can significantly mitigate energy losses associated with power curtailment, which occurs when generation exceeds demand [6]. Consequently, this can enhance system efficiency and economic viability by reducing the need for excessive capacity in both energy production and electrical storage [7]. Furthermore, hydrogen's versatility extends beyond mere energy storage, encompassing a range of grid support services such as contingency response and load-following [8]. These characteristics are essential to managing the intrinsic variability of renewable energy sources (VREs) like solar and wind, whose intermittent nature prevents them from reliably meeting energy demand without supplementary solutions [9,10].

In this context, hydrogen is central to facilitating the integration of a growing share of VREs, aligning with national and international decarbonization strategies [11]. Higher penetration of VREs can enhance

* Corresponding author.
E-mail addresses: d.vizza@lab.unimarconi.it (D. Vizza), r.caponi@lab.unimarconi.it (R. Caponi), e.bocci@unimarconi.it (E. Bocci), luca.delzotto@uniecampus.it (L. Del Zotto), claudia.bassano@enea.it (C. Bassano).

https://doi.org/10.1016/j.ecmx.2025.101136
Received 4 January 2025; Received in revised form 27 June 2025; Accepted 3 July 2025
Available online 9 July 2025
2590-1745/© 2025 The Author(s). Published by Elsevier Ltd. This is an open access article under the CC BY license (http://creativecommons.org/licenses/by/4.0/).

Nomenclature

h	Convective heat transfer coefficient, W/m^{2}K
Hop	Operational hours
i	Component
idx	Index
k	Thermal conductivity, W/mK
L	Tank heigh, m
N	Project lifetime
P	Power, kW
r	Radius, m
R	Resistance, K/W
Rl	Remaining lifespan
Sls	Total stack lifespan
Sr	Salvage revenue
z	Interest rate

Acronyms

AEL	Alkaline
AEM	Anion exchange membrane
BoP	Balance of plant
CAPEX	Capital cost of expenditure
DC	Direct current
ELE	Electrolyzer
EOL	End-of-life
ETS	Emissions Trading System
EU	European Union
H2	Hydrogen
IPCEI	Important Projects of Common European Interest
KOH	Potassium hydroxide
LCOH	Levelized cost of hydrogen
LHV	Low heating value
NPC	Net present cost
OPEX	Operational cost of expenditure
PEM	Proton exchange membrane
PtG	Power-to-gas
PV	Photovoltaic
PVGIS	Photovoltaic geographical Information system
REP	Replacement
SEC	Specific energy consumption
VRE	Variable renewable energy

Subscripts

aux	Auxiliaries
c	Conversion
cond	Conduction
conv	Convection
deg	Degradation
ext	External
int	Internal
nom	Nominal
tot	Total

energy affordability by reducing electricity prices, which in turn lowers the production costs of green hydrogen [12]. However, this reduction in electricity prices could also lead to a decline in wholesale electricity revenues, potentially affecting the economic viability of VRE plants [13]. To mitigate such risks, a hybrid system incorporating hydrogen offers both technical and economic advantages. It provides flexibility for investors and operators to optimize returns, either by selling electricity at market rates or converting surplus electricity into hydrogen when generation costs are low, thus enhancing the overall financial sustainability of renewable energy projects [14].

Continued research and development are essential to integrate these emerging energy systems with existing infrastructure and to identify the most profitable transition strategies for widespread adoption. Numerous studies have been proposed in the literature, focusing on projected cost reductions and improvements in conversion efficiency for hydrogen production. Comprehensive technical evaluations have been conducted on different power-to-gas (PtG) technologies, including steam methane reforming [15,16], wind-based electrolysis [17,18], photovoltaic (PV) systems coupled with electrolysis [19,20] and grid electrolysis [21,22]. Research has also explored the integration of battery storage [23,24] and the combination of renewable sources with grid connections [25,26].

Additionally, comparative studies on water technologies, both in relation to other hydrogen production processes [27], and across different electrolyzer types [28], provide valuable insights into their respective advantages and limitations. While some research emphasizes the need for further technological advancements to strengthen hydrogen's role in sustainable and renewable energy systems [29], others highlight that its widespread adoption is less constrained by technical barriers and more by the requirement for continuous investment to achieve the necessary scale [30]. In line with this, many studies have addressed the economic viability of hydrogen systems. For instance, Roach and Meeus [31], investigated the price effects of sector coupling with PtG, with the technology expected to become more cost-effective and efficient, as indicated by Glenk et al. [32]. Marzi et al. [33] examined the operational strategies for PtG solutions, including both generation and price uncertainties in their model. Additionally, Blanco and Faaij [34] explored the role of PtG technologies within the broader global energy system. The economic sustainability of PtG is also the subject of studies focused on the transport sector, which has been more recently addressed for both heavy-duty [35] and light-duty applications [36].

In order to facilitate widespread adoption and achieve economies of scale for electrolysis-based hydrogen production systems, the European Union (EU) has introduced a range of support programs [37]. These initiatives target the entire hydrogen value chain, from electrolyzer manufacturing to retail distribution networks. Notably, four waves of hydrogen-related Important Projects of Common European Interest (IPCEI) have been approved, amounting to EUR 18.9 billion [38]. Furthermore, the EU Hydrogen Bank provides additional support by issuing tenders designed to offer a fixed premium for renewable hydrogen production, covering both domestically produced and imported supplies.

Electrolyzer deployment also benefits from support under calls for proposals in the EU "Innovation Fund," financed through the Emissions Trading System (ETS). Furthermore, many European countries have chosen to allocate portions of the NextGenerationEU and REPowerEU funds to finance electrolytic hydrogen production initiatives, resulting in the emergence of numerous hydrogen valleys across the continent.

In the long run, these funding programs, by improving the profitability of hydrogen production, increasing the cost-effectiveness of hydrogen adoption, and supporting the development of a dedicated distribution network, seek to foster the creation of a new market. In doing so, they address adoption barriers, including those associated with technology lock-in, and ultimately help align previously latent demand with potential supply [39].

Given these developments, the present study focuses on the techno-economic modeling of solar-driven electrolysis systems for hydrogen production in stand-alone configurations. A critical component of this modeling involves determining the optimal ratio between PV capacity and electrolyzer nominal power (PV:ELE), aiming to minimize both capital expenditure and operational costs. Yates et al. [40] identified the

size of the electrolyzer system as a key determinant of the levelized cost of hydrogen (LCOH). Sayedin et al. [41] further demonstrated that climatic conditions play a significant role in determining the optimal electrolyzer size and the resulting LCOH. In addition, Marocco et al. [42] observed an inverse relationship between the utilization factors of the electrolyzer and the PV generator, suggesting that maximizing electrolyzer efficiency may not always align with optimizing PV output. Hassan et al. [43] further confirmed that multiple cost-competitive configurations exist for systems operating within renewable hydrogen markets. Lastly, Yang et al. [44] illustrated that employing more accurate and refined PV production models can significantly improve annual profits by minimizing inefficiencies and enhancing energy production forecasts.

To date, most studies have primarily focused on global analyses to identify general optimal configurations and project potential LCOH trajectories, as detailed by Grüger et al. [45] and Jamshidi and Askarzadeh [46]. However, such approaches often lead to generalized and non-specific cost estimations, resulting in less precise evaluations of hydrogen production. The proposed work seeks to refine LCOH estimation by proposing an evaluation approach that leverages on detailed simulations of electrolyzer operation, including thermal management of the electrolyte, start-up procedure simulation, and ultimately, stack usage optimization. To bridge the research gaps, this study introduces a modified in-house MATLAB algorithm designed to evaluate various operational strategies, with a particular effort on quantifying the impact of stack replacement at end-of-life and the benefits of alternating stack operation to enhance overall system efficiency through uniform utilization of individual stack elements. Additionally, a comparison with alternative control strategies for electrolyzer operation is presented.

The paper is organized in the following structure: Following the introduction, Section 2 illustrates the equations used within the model and provides a description of the type of system analyzed. Section 3 delves into the key findings of the model assessing the optimal PV:ELE ratio in different locations as well as the impact of different stack management strategies on the LCOH. The paper concludes by summarising the most relevant results and reflecting on the implications for future research.

2. Modeling framework

2.1. Model equations

To achieve the declared objectives an economic simulation has been developed in MATLAB based on the definition of LCOH as the ratio between the net present value of the total cost occurred during the project lifetime (N) actualized at a constant interest rate (z), also known as net present cost (NPC), and the actualization at the same constant interest rate of the hydrogen produced ($H2_{prod,n}$) during the same timeframe.

$$LCOH = \frac{NPC}{\sum_{n=1}^{N}\left[H2_{prod,n} \bullet (1+z)^{-n}\right]} \tag{1}$$

The NPC is defined as the sum of capital expenditure (C_{apex}) and the actualized value of the yearly operational expenditure (C_{opex}) for each element of the system (i). The latter includes a fixed operational cost component estimate as a percentage of the C_{apex}, a variable component linked to the stack replacement simulation and, during the last year of operation, a salvage revenue derived from the residual lifetime of the electrolyser stack.

$$NPC = \sum_{i}\left[C_{apex,i} + \sum_{n=1}^{N}\frac{C_{opex,i,n}}{(1+z)^{n}}\right] \tag{2}$$

Optimizing production through the selection of the most suitable PV configuration and accurately assessing near end-of-life (EOL) power consumption are critical factors in enhancing operational performance and, consequently, reducing the LCOH. Additionally, the LCOH can benefit from a proper assessment of salvage revenue at the end of the project's lifetime. However, establishing the residual value of the electrolyser stack at the end of its lifecycle poses considerable challenges due to uncertainties in stack degradation rates and operational conditions. The proposed model addresses these challenges by providing precise predictions of the electrolyser's remaining lifespan $Rl_{i,20}$, defined as the difference between the operational hours at the end of last year, $Hop_{i,20}$, and the total stack lifespan over the total stack lifespan, Sls_i. This calculation is made possible by detailed simulations of cumulative operating hours at stack level.

$$Rl_{i,20} = Hop_{i,20} - Sls_i \tag{3}$$

In the proposed model the salvage revenue, Sr, from the electrolyzer stack is evaluated as the ratio of the remaining operational hours, $Rl_{i,20}$, and the total stack lifespan over the total stack lifespan, Sls_i, multiplied by the original stack cost, $C_{apex,stack}$.

$$Sr = \sum_{i}\left[\frac{Rl_{i,20}}{Sls_i} \bullet C_{apex,stack}\right] \tag{4}$$

Potential electricity sales revenues were intentionally excluded as a positive component in Eq. (2). This approach ensures that the LCOH is not artificially underestimated due to the revenue potentially generated by photovoltaic installations. All the economic parameters used in the model for the determination of the LCOH for each system component, along with the corresponding literature references, are presented in Table 1.

2.2. System configuration

As clearly evident in Eq. (1), computing the LCOH calculations fundamentally depends upon establishing hydrogen production throughout the plant's operational period. More specifically, the correspondence of the LCOH quantification with respect to the actual costs that can be incurred in implementing green hydrogen production systems is intrinsically associated with the accuracy with which the hydrogen quantity from the integrated PV-electrolyzer system is modeled. To address the growing market need for realistically reflecting

Table 1
Economic assumptions utilized as an input in the presented model for the calculation of the LCOH.

Component/ Parameter	Data/Value	Ref
Solar photovoltaic		
$CAPEX_{fixed}$	650 €/kW	2024 market analysis*
$CAPEX_{tracker}$	700 €/kW	2024 market analysis*
OPEX	2 % (% of CAPEX)	[46]
Decay	1 % first year; 0.3 % each year	Based on manufacturer data
Lifetime	20 years	[45]
DC/DC converter		
CAPEX	70 €/kW	[47]
Lifetime	20 years	[45]
Electrolyzer		
CAPEX	1,144 €/kW	2024 market analysis*
OPEX	2 % (% of CAPEX)	[48]
REPLEX	45 % (% of CAPEX)	[49]
Decay	0.4 % over 1000 h of operation	Based on manufacturer data
Lifetime	20 years	[45]
Economic assumptions		
Fixed discount rate	6 %	[14]

* The market analysis was conducted through individual interviews.

the actual operational conditions of these innovative yet increasingly spreading systems, the authors previously developed an advanced 1 MW electrolyzer model. This is designed to simulate the operation of a commercially available AEM (anion exchange membrane) electrolyzer and was developed using publicly available data provided by the manufacturer, while thoroughly analyzing and modelling its operational behaviour. The integration of solar energy production and hydrogen generation is conducted on an hourly basis over the entire lifetime of the plant, which has been assumed to be 20 years based on the studies and simulations conducted on AEM electrolyzers by Kim et al. [49].

Given the intrinsic intermittency of solar irradiation, it requires a production model capable of coping with fluctuations in operational states, such as transitions from inactive to active phases, and adjustments in operating parameters such as temperature and pressure. This study makes use of these parameters to determine the electrolyzer's operating conditions and, consequently, to assess hydrogen production through the application of efficiency curves associated with the various system components.

Within this model, the hydrogen output is derived starting from the incident solar irradiance on photovoltaic panels, converting the corresponding energy into electricity while accounting for annual panel degradation (Eq. (5)) and incorporating efficiency losses due to the power conversion systems (Eq. (6)):

$$P_{PV,deg} = P_{PV} \bullet (1 - 0.01 - (0.003 \bullet \text{years})) \quad (5)$$

$$P_{PV,H2} = P_{PV,deg}(idx) \bullet \eta_c \quad (6)$$

The panel degradation is implemented according to the current most advanced, yet commercial, technology (i.e. silicon heterojunction solar cells) indications, which consider a 1 % reduction in nominal power output during the first year of operation followed by a linear a linear degradation rate of 0.3 % annually. After comprising for the load-dependent conversion efficiency, η_c, the power available for hydrogen production is represented by $P_{PV,H2}$. The model considers crystalline silicon solar panels since it is the predominant technology of global PV production [50] and two different mounting configurations:

- Conventional, fixed installation with optimized inclination and footprint based on installation location.
- Horizontal monoaxial sun tracker systems, with dynamically variable azimuthal angle and optimized surface footprint on installation location.

Furthermore, the electrolyzer's operation has been modelled to enable an accurate simulation of the start-up procedure, including both the energy and the time required to bring the system to the optimal temperature and pressure operational conditions.

AEM electrolyzer technology has been employed for hydrogen generation in this model due to its favourable compatibility with VRE sources and its capacity to operate under flexible conditions. Compared to other widely adopted technologies like PEM (proton exchange membrane) electrolyzers, AEM allows to overcome the problem of dependency on rare materials, while maintaining a compact footprint and mitigating corrosion issues commonly present in AEL (alkaline electrolyzers) units [51].

The modeled AEM accounts for 42 stacks, each with a nominal power of 22.91 kW divided into two equal sets. Each set, which can operate independently, absorbs about 500 kW at the beginning of life including the auxiliaries and features an electrolyte tank containing 1,000 L of an aqueous solution with a 1 % w/v potassium hydroxide (KOH) concentration.

The MATLAB simulation is able to evaluate the operational hours of each stack, determining the expected degradation level and associated electrical consumption. Based on this assessment, the least degraded stacks are sequentially selected to maximize the efficiency of hydrogen generation. Combined with information about string operational hours, replacement intervals, and the available lifespan at the project's end-of-life, it represents key elements in the precise evaluation of LCOH. Table 2 presents the technical specifications of each component used as an input parameter in the model.

2.3. Simulation algorithm

Fig. 1 shows the functional logic scheme describing the algorithm developed in this paper aiming to define the LCOH, expressed in €/kg, for different combinations of PV:ELE power ratio (q) identifying the cost-optimal configuration over a 20-year investment period (i). The algorithm simulates, hour-by-hour, the interchange between PV production, and electrolyzer operation, including thermal management and stack-level effects, and economic parameters. If the following condition is verified:

- $P_{PV} > 0$ $(daytime)$

The algorithm accomplishes the subsequent three main actions:

- *Step 1*: identification of the PV power output at each stack level taking into consideration the solar hourly meteorological data, including the effects of PV system degradation. Within each hour, the algorithm evaluates whether the available PV power is sufficient to supply the auxiliary loads necessary for the electrolyzer transition to operational state – defined as the condition where the electrolyte temperature reaches the threshold of 35 °C – and, subsequently, whether the remaining power can be allocated to hydrogen production. The model explicitly represents intermediate conditions such as the hot standby condition, in which the electrolyzer is maintained at an intermediate temperature below its maximum operating temperature, and the cold standby condition, during which prolonged inactivity necessitates a full pre-heating sequence before starting the production. The simulation considers the two electrolyzer sets, whose activation is dynamically managed based on real-time PV power availability and electrolyte thermal conditions. The operational logic of the system is highly responsive to the variability of solar energy input, enabling a non-sequential and adaptive control strategy that ensures optimal use of available energy.
- *Step 2*: evaluation of the cumulative operational hours of each individual stack and therefore of the relative consumption and degradation. To achieve a uniform distribution of the stacks' utilization and maximize their efficiency, a non-sequential activation logic is simulated. At the end of each operational cycle, the stacks are ranked

Table 2
Main technical features of the system components.

Component/Parameter	Data/Value
*Solar photovoltaic-Risen Energy**	
η_{PV}	22.5 %
$P_{PV,module}$	700 W
Decay	1 % first year; 0.3 % each year
DC/DC converter-Epic Power	
η_{c1}	85 % (input power 0 %–20 %)
η_{c2}	90 % (input power 20 %–40 %)
η_{c3}	98 % (input power 40 %–100 %)
*Electrolyzer-AEM multicore**	
$P_{set,nom}$	1008 kW
$P_{single,stack}$	22.91 kW
N_{stack}	42
P_{aux}	45.78 kW
SEC_1	4.5 kWh/Nm^3 (stack efficiency load 3 %–30 %)
SEC_2	4.6 kWh/Nm^3 (stack efficiency load 3 %–30 %)
SEC_3	4.4 kWh/Nm^3 (stack efficiency load 3 %–30 %)

* Note: based on 2024 data.

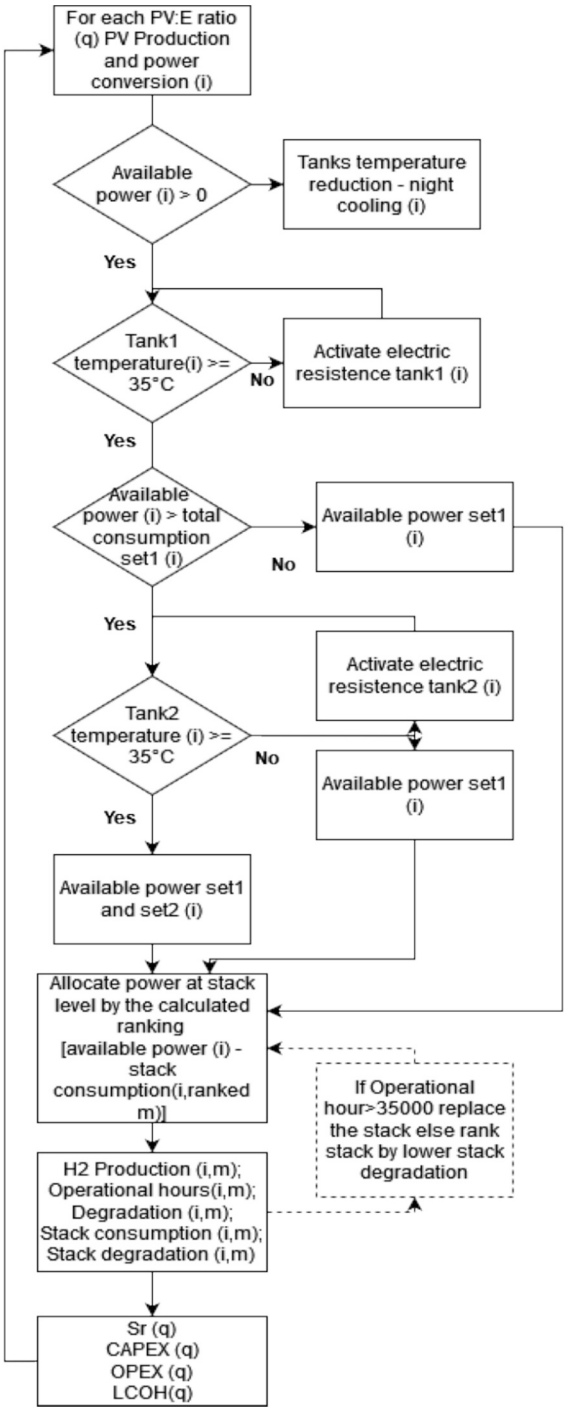


Fig. 1. Flow chart of the developed model, illustrating the operational logic that leads to the evaluation of the hydrogen production costs.

and reordered, ensuring power is preferentially allocated to the least degraded. In this step it is also derived the hydrogen produced according to the relation $m_{H2} = \left(P_{ELE} - P_{stack.loss}\right) \bullet \eta_{stack}/LHV_{H2}$.

- *Step 3*: calculation of the actualized CAPEX, OPEX and salvage revenues as indicated in Eqs. (2) and (3). Finally, the algorithm computes the LCOH for each tested PV:ELE ratio. Hence, it obtains a matrix of LCOH values and identifies the optimal system configuration that minimizes the hydrogen production cost.

In the case the following condition is met:

- $P_{PV} = 0$ $(nighttime)$

The proposed algorithm simulates the thermal losses that occur overnight due to the temperature differential between the electrolyte solution and the ambient environment. This temperature gradient drives conductive heat transfer through the tank walls and convective heat exchange with the surrounding air. By quantifying these mechanisms, the model determines the electrolyte's temperature at the start of each subsequent day. For a cylindrical vessel, the overall thermal resistance (in K/W) governing these heat transfer processes is given by:

$$R_{tot} = R_{cond} + R_{conv} = \frac{\ln(r_{ext}/r_{int})}{2\pi \bullet L \bullet k} + \frac{1}{2\pi \bullet r_{ext} \bullet L \bullet h_{air}} \quad (7)$$

where r_{ext} and r_{int} the external and internal tank radius, respectively; L is the tank height; k is the thermal conductivity of the insulating layer (0.035 W/mK); h_{air} is the heat transfer for still air (25 W/m^2 K).

2.4. Management strategies for stacks replacement

The developed model, focusing on the operational performance of individual stacks as a key element of the simulation, raises significant questions about optimal strategies for the management of their availability. Specifically, the above-defined strategy, which involves replacing stacks upon reaching the end of their useful life and alternating their operation to maximize overall system efficiency at any given time, implies a homogeneous utilization of individual elements. However, alternative usage strategies can be envisioned, and their impacts are analysed in this study.

In particular, the algorithm described above has been modified in step 2 in the following three ways:

1) Alternative 1 – No optimization in stack usage: the stacks were operated sequentially based on their numerical order, utilizing the power available from the PV system, and were replaced at the end of their useful life.
2) Alternative 2 – Stack replacement at year 10 (half of the plant lifetime): Stacks were operated ranked by their degradation levels, prioritizing the least degraded ones. However, the stacks were replaced after reaching half of the assumed plant lifetime.
3) Alternative 3 – Stack segregation to reduce replacements: Stacks were operated based on their degradation levels, with a variable number of stacks segregated and operated as a distinct set whenever the power saturation of the main set was reached. Replacements occurred at the end of the stacks' useful life.

These four defined strategies were integrated into step 3 to evaluate their impact on the LCOH.

2.5. Simulation conditions

As highlighted by Yates et al. [40], the ratio between PV capacity and electrolyser rating exerts a decisive influence on the resulting LCOH under varying irradiance conditions. Their Monte Carlo-based simulation indicates that cost-effective solutions tend to cluster around a 1.5:1 PV:ELE ratio. Consequently, the developed simulation model has been iteratively run with a variable ratio between PV and electrolyser nominal power ranging from 1:1 to 2:1 with steps of 0.1, with six different sets of PV irradiance derived from Photovoltaic Geographical Information System software (PVGIS).

The sites were selected based on their potential interest in hydrogen production, namely the Hamburg district in northern Germany, the Civitavecchia district in central Italy, and Zuara in northern Libya. The first two locations are characterized by significant port infrastructure with extensive interconnections to both the national electricity grids and gas networks [52,53]. Additionally, both districts could benefit from

hydrogen availability as part of efforts to decarbonize human activities related to maritime transportation [54]. The third location, Zuara, was chosen due to its proximity to the Greenstream pipeline, which links Libya to Italy [55].

For each location a set of two different twenty-year long total irradiation datasets have been extracted from PVGIS, the first has been acquired by selecting a fixed mounting configuration optimized in its tilt and the second has been acquired by choosing a monoaxial tracking mounting configuration. These data allowed us to simulate the entire life horizon of the system with an hourly definition.

3. Results and discussion

The simulation algorithm described in Section 2.3, with its three fundamental steps, was applied under the simulation conditions outlined in Section 2.5. The following sections present the results of the analyses conducted (Section 3.1) and discuss the variables that conditionate the PV:ELE optimal ratio (Section 3.2). Additionally, an evaluation of the stacks' utilization as well as the impacts of the alternative stack usage strategies defined in Section 2.4 will be provided (Section 3.3).

3.1. LCOH result simulation analysis

Table 3 presents the simulation results for the LCOH, including the essential parameters and variables utilized in its calculation as detailed in the equations presented in Section 2.1. The table also identifies the optimal PV:ELE ratios corresponding to the lowest LCOH values across the six simulated scenarios described in Section 2.5. In assessing the optimal sizing for PV systems, the simulation results underscore that both oversizing and undersizing negatively impact the LCOH, though the impact varies. Specifically, an oversizing of 0.3 MW for installations in Civitavecchia increases the LCOH by 1.4 % for fixed systems and 1.6 % for trackers, whereas the same oversizing in Zuara leads to greater increases of 2.1 % and 2.9 %, respectively. Conversely, undersizing by 0.3 MW in Civitavecchia results in even higher LCOH increments, reaching 2.1 % for fixed systems and 3.9 % for tracker systems. In contrast, Zuara, experiences relatively lower impacts from undersizing, with LCOH increments of 1.4 % for fixed and only 0.5 % for trackers. Finally, in the Hamburg region, undersizing by 0.2 MW increases the LCOH by 1.2 % for fixed configurations and marginally by 0.2 % for trackers, while equivalent oversizing results in modest LCOH increases of 0.3 % and 1 %.

Fig. 2 provides a detailed color-map visualization of the simulated LCOH values corresponding to various PV:ELE ratios, clearly illustrating the relationship between system configuration, location, and hydrogen production economics. The optimal lowest LCOH value of 4.47 €/kg is achieved in Zuara using the tracking configuration, representing the most cost- effective scenario analyzed. Conversely, the highest LCOH, reaching 7.50 €/kg, occurs in Hamburg with a fixed PV configuration. It is noteworthy that the optimal LCOH values for fixed PV installations in Zuara and Civitavecchia are closely comparable. The analysis of cost distribution across the various locations highlights the electrolyser CAPEX as the predominant factor influencing the LCOH (see Fig. 3). Additionally, it is noted that when the stack replacement occurs near the conclusion of its projected lifespan, it has accumulated relatively few operational hours, thus retaining substantial residual market value.

Fig. 4 provides a detailed representation of the monthly average hydrogen production values obtained from the 20-year simulation period, comparing the three selected locations and the two photovoltaic mounting configurations, each evaluated at their optimal PV:ELE ratio as identified in Table 3. Despite utilizing a photovoltaic system with a nominal capacity twice that of the electrolyzer, the expected production from an installation in the Hamburg district in northern Germany (Lat. 53°34′ N) is over 35 % lower than that of an identical configuration installed in Zuara, northern Libya (Lat. 32°56′ N) while examining the tracking system. Consequently, a 1 MW monoaxial tracking system in Zuara produces an amount of hydrogen equivalent to a 2 MW system installed in Hamburg. Similarly, when comparing installations, the production in the Civitavecchia district in central Italy (Lat. 42°06′ N) is 16 % lower than in Zuara. Table 4 summarizes these insights, illustrating the annual average hydrogen production data. It highlights the performance advantages offered by the tracking solution. By continuously optimizing the incidence angle of solar irradiation throughout the day, the tracking system achieves a higher overall yield compared to fixed installations. This advantage is especially evident in Zuara, where the tracking configuration results in a 17 % increase in hydrogen output compared to fixed mounting. This advantage is particularly pronounced in Zuara, where the tracker configuration increases hydrogen output by approximately 17 % compared to fixed installations.

Fig. 5 and Table 5 further underscore this performance differential by presenting the energy output of a 1 MWp PV installation across different locations throughout the analyzed period. Although the main differentiating factor among the selected locations undoubtedly lies in the average solar irradiation —directly affecting overall energy yield—it is important to note that ambient temperature, if not properly accounted for, can also impact the site's productivity.

As previously stated, hydrogen production commences only once the electrolyte temperature reaches 35 °C, the minimum operating threshold. The AEM electrolyzer considered in this work runs at 55 °C, which is not far from the maximum allowable temperature beyond which the system must be halted. Consequently, installations located in extreme climates require specific adaptations to the BoP that, rather than altering the production potential, can result in comparatively higher installation costs.

3.2. PV to electrolyser optimal ratio

The results, discussed in Section 3.1 highlight that the optimal ratio between PV:ELE nominal power able to minimize the LCOH is dependent on the geographical location of the installation and the related solar irradiance as well as on the system configuration selected.

- Geographical Variations:
  - **Hamburg – Northern Germany**: This northern location characterized by relatively low solar irradiance and a reduced number of equivalent hours, requires a higher-capacity PV installation to meet the energy demand of a 1 MW electrolyzer. Consequently, the optimal PV:ELE capacity ratio is determined to be 1.8:1. The combined effect of reduced hydrogen production and elevated CAPEX results in a higher LCOH compared to the optimal configurations observed at other locations. Beyond this optimal threshold, the marginal increase in hydrogen production fails to offset the additional CAPEX, making further investment less cost-effective.
  - **Civitavecchia – Central Italy**: Central Italy benefits from a higher solar irradiance and a more balanced seasonal profile than Hamburg. The milder seasonal variations translate to better year-round utilization of the PV-ELE system, allowing a lower sizing ratio, that is between 1.5:1 and 1.6:1, depending on the specific installation type. These findings are consistent with literature recommendations for regions with moderate solar resources, confirming their suitability for such configurations.
  - **Zuara – Northern Libya**: Although Libya's high solar irradiance might suggest a lower optimal ratio, the analysis indicates that an optimal ratio of 1.6:1, similar to that in Italy, is most effective. Nevertheless, the significantly high capacity factor for both PV and electrolyzer, substantially lowers the LCOH, primarily due to the increased hydrogen production enabled by the abundant solar resources. This enhanced output offsets capital and operational costs, making installations in this region more economically favourable.

Table 3
Simulation results in the 3 selected sites considering different PV mounting solutions and PV:ELE ratios, in which it is also evidenced the optimal ratio for each configuration that achieves the lowest LCOH.

RESULTS CENTER-ITA											
Ratio PV:ELE	1	1.1	1.2	1.3	1.4	1.5	1.6	1.7	1.8	1.9	2
LCOH (€/kg) – fixed axes	6.56€	6.20€	5.95€	5.80€	5.73€	5.71€	5.69€	5.71€	5.73€	5.76€	5.83€
Total H2 production (kg) 20 years	601,688	665,271	729,007	782,147	826,162	862,804	895,467	924,279	949,421	971,374	991,622
H2 prod actualized (kg)	348,493	384,952	420,151	449,674	474,335	495,049	513,588	529,975	544,268	556,832	568,416
Stack replacement time (year)	0	19	18	17	16	15	15	14	14	14	13
CAPEX (€)	1,873,152€	1,945,152€	2,017,152€	2,089,152€	2,161,152€	2,233,152€	2,305,152€	2,377,152€	2,449,152€	2,521,152€	2,593,152€
OPEX + REP actualized (€)	413,640€	592,271€	617,005€	642,329€	668,277€	694,887€	709,798€	737,111€	752,022€	766,932€	794,989€
Salvage actualized (€)	-€	148,839.17€	134,172.46€	122,007.05€	112,016.48€	103,588.72€	96,114.78€	89,544.13€	83,828.65€	78,795.69€	74,106.74€
LCOH (€/kg) - tracker 1-x	5.69€	5.43€	5.21€	5.09€	5.04€	5.02€	5.04€	5.06€	5.10€	5.17€	5.27€
Total H2 production (kg) 20 years	726,378	805,997	882,071	945,665	995,220	1,036,697	1,070,611	1,101,090	1,127,771	1,150,948	1,171,719
H2 prod actualized (kg)	419,268	464,034	507,058	542,964	571,155	594,752	614,182	631,554	646,788	660,060	671,931
Stack replacement time (year)	18	16	15	14	13	13	12	12	12	11	11
CAPEX (€)	1,923,152€	2,000,152€	2,077,152€	2,154,152€	2,231,152€	2,308,152€	2,385,152€	2,462,152€	2,539,152€	2,616,152€	2,693,152€
OPEX + REP actualized (€)	598,653€	636,161€	663,919€	692,378€	721,582€	737,639€	767,632€	783,690€	799,747€	830,576€	846,634€
Salvage actualized (€)	134,460€	115,837€	98,232€	83,850€	72,670€	63,237€	55,549€	48,588€	42,542€	37,241€	-€

RESULTS NORTH-GER											
LCOH (€/kg) – fixed axes	9.17€	8.66€	8.38€	8.07€	7.85€	7.70€	7.59€	7.55€	7.50€	7.51€	7.53€
Total H2 production (kg) 20 years	423,207	467,356	509,396	547,402	581,776	613,071	641,515	669,756	696,094	720,138	742,385
H2 prod actualized (kg)	243,865	269,510	293,769	315,623	335,410	353,390	369,735	385,488	400,158	413,650	426,185
Stack replacement time (year)								19	19	18	17
CAPEX (€)	1,873,152€	1,945,152€	2,017,152€	2,089,152€	2,161,152€	2,233,152€	2,305,152€	2,377,152€	2,449,152€	2,521,152€	2,593,152€
OPEX + REP actualized (€)	413,640€	428,551€	443,462€	458,373€	473,284€	488,195€	503,106€	681,736€	696,647€	721,381€	746,705€
Salvage actualized (€)	51,191.94€	40,825.43€	-€	-€	-€	-€	-€	148,556.74€	142,481.18€	136,894.51€	131,781.07€
LCOH (€/kg) - tracker 1-x	8.26€	7.78€	7.39€	7.10€	6.93€	6.84€	6.80€	6.80€	6.79€	6.83€	6.86€
Total H2 production (kg) 20 years	493,102	543,790	593,906	641,192	687,064	725,833	758,976	788,846	815,504	839,352	860,732
H2 prod actualized (kg)	284,416	313,949	343,122	370,317	395,384	416,887	435,522	452,314	467,364	480,926	493,164
Stack replacement time (year)					19	18	17	16	16	15	15
CAPEX (€)	1,923,152€	2,000,152€	2,077,152€	2,154,152€	2,231,152€	2,308,152€	2,385,152€	2,462,152€	2,539,152€	2,616,152€	2,693,152€
OPEX + REP actualized (€)	425,110€	441,168€	457,226€	473,284€	653,062€	678,943€	705,413€	732,508€	748,566€	776,324€	792,382€
Salvage actualized (€)	-€	-€	-€	-€	144,230€	135,373€	127,791€	120,942€	114,842€	109,373€	104,473€

RESULTS NORTH-LIB											
LCOH (€/kg) – fixed axes	5.77€	5.49€	5.28€	5.16€	5.10€	5.09€	5.08€	5.12€	5.15€	5.19€	5.24€
Total H2 production (kg) 20 years	690,631	766,977	836,997	896,216	944,829	984,718	1,018,486	1,048,017	1,073,747	1,096,298	1,116,340
H2 prod actualized (kg)	400,104	442,862	482,242	515,546	542,978	565,577	584,797	601,614	616,280	629,153	640,631
Stack replacement time (year)	19	17	16	15	14	13	13	12	12	12	12
CAPEX (€)	1,873,152€	1,945,152€	2,017,152€	2,089,152€	2,161,152€	2,233,152€	2,305,152€	2,377,152€	2,449,152€	2,521,152€	2,593,152€
OPEX + REP actualized (€)	577,360€	612,507€	638,455€	665,066€	692,378€	720,435€	735,345€	764,191€	779,102€	794,013€	808,923€
Salvage actualized (€)	142,841€	125,018€	108,892€	95,444€	84,381€	75,330€	67,631€	60,912€	55,083€	49,945€	45,337€
LCOH (€/kg) - tracker 1-x	4.99€	4.75€	4.59€	4.49€	4.46€	4.48€	4.47€	4.51€	4.55€	4.60€	4.67€
Total H2 production (kg) 20 years	850,903	940,268	1,022,768	1,092,350	1,149,179	1,195,431	1,233,053	1,263,772	1,289,315	1,310,729	1,329,167
H2 prod actualized (kg)	490,772	541,785	588,791	628,324	660,681	686,966	708,367	725,812	740,278	752,390	762,635
Stack replacement time (year)	15	14	13	12	11	11	11	10	10	10	10,20
CAPEX (€)	1,923,152€	2,000,152€	2,077,152€	2,154,152€	2,231,152€	2,308,152€	2,385,152€	2,462,152€	2,539,152€	2,616,152€	2,693,152€
OPEX + REP actualized (€)	631,803€	660,262€	689,466€	719,458€	750,286€	766,344€	782,402€	814,117€	830,175€	846,232€	1,016,743€
Salvage actualized (€)	105,317€	84,453€	65,485€	49,660€	36,826€	-€	-€	-€	-€	-€	150,849€

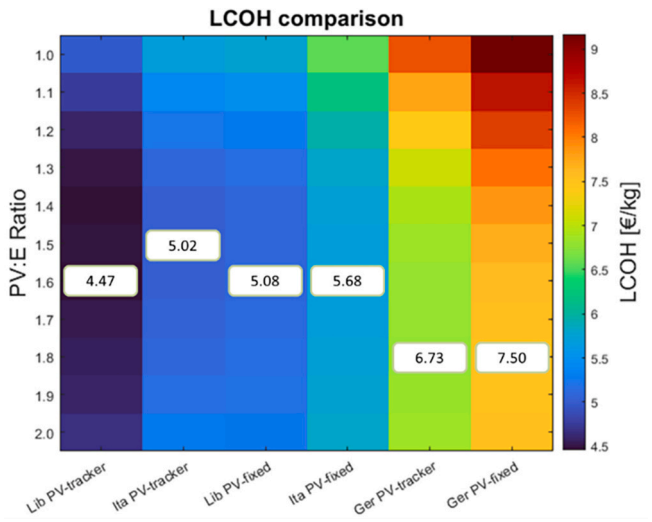


Fig. 2. Map chart of the LCOH in the 3 selected sites considering different PV setup and PV:ELE ratio, evidencing the minimum LCOH for each configuration.

- System-Level Trade-offs:
  - **PV configuration impact:** Tracking systems prove beneficial across all analyzed regions, albeit with varying degrees of effectiveness. In Libya, tracking systems lead to a significant LCOH reduction of 12 %, while in Italy and Germany, the reduction is 11.3 % and 10.2 %, respectively.

    This analysis underscores that the additional CAPEX of 50 €/kW for tracking systems is well justified across all scenarios, particularly in regions with higher solar resource availability, where the relative advantages are more significant. The installation of monoaxial trackers leads to a reduction in the LCOH for the optimal configuration of 12 % in Zuara, 11.8 % in Civitavecchia, and 9.5 % in Hamburg. This reduction is primarily driven by location-specific irradiance patterns, which enhance the performance and efficiency of tracking systems. In addition to increasing total energy production, as illustrated in Fig. 5, tracking systems significantly alter the production profile, as detailed in Fig. 6. Unlike fixed mounting systems, tracking systems extend the hours of substantial power output by capturing more energy during the early morning and late afternoon periods.

    Table 6 presents the average number of equivalent hours for both the photovoltaic system and the electrolyzer. Analyzing the percentage changes shows that, in regions located farther north, the increase in the electrolyzer's equivalent hours exceeds the corresponding gain in photovoltaic equivalent hours.

    However, this comes at the cost of a slight reduction in midday peak production, as the system prioritizes a more balanced energy capture throughout the day rather than maximizing peak output. This reconfiguration of the production curve better aligns with the operational characteristics of the electrolyzer, enhancing its utilization ratio and ultimately driving the observed reductions in LCOH, despite the minor trade-off in peak performance.
  - **Curtailment power and replacement costs**: An excessively high PV:ELE ratio can lead to substantial overproduction of electricity during mid-day hours, resulting in increased curtailment of power. Moreover, the enhanced energy availability during winter months may lead to higher overall electrolyzer utilization. While this might seem like a positive outcome, it is important to consider that, under certain circumstances, this can result in the need for an additional stack replacement toward the end of the system's lifetime. This, in turn, may introduce costs that are not fully offset by the extra hydrogen production. This issue is particularly significant in regions with high solar irradiation levels.

3.3. *Utilization of the stacks and alternative management control logic*

Section 2.4 introduced the conceptual framework for evaluating various management strategies for stack replacement. In this section, we present an analysis of the operational outcomes associated with these approaches:

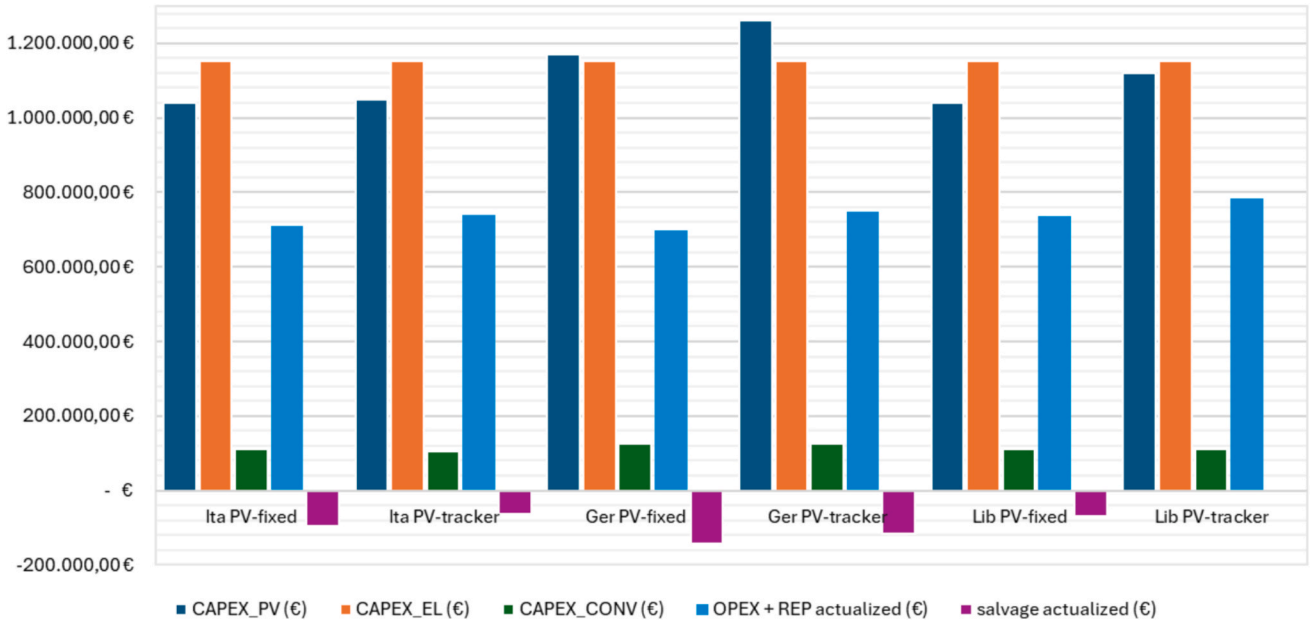


Fig. 3. Breakdown of the LCOH for each configuration analysed for their optimal PV:ELE ratio.

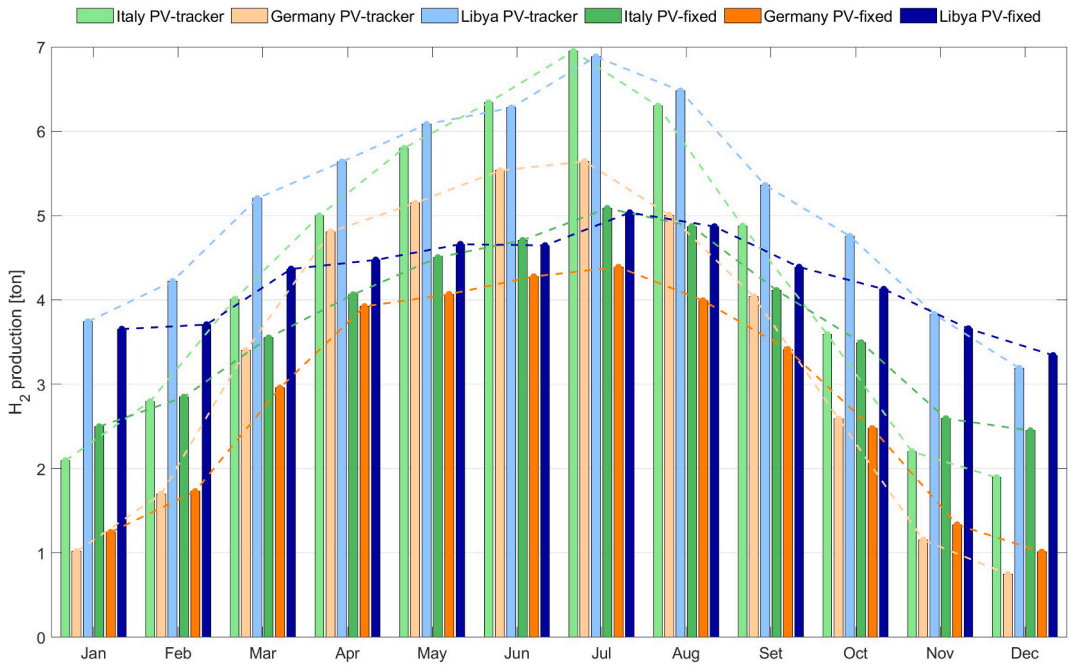


Fig. 4. Average monthly hydrogen production over the 20-year lifespan for the three sites and two PV mounting configurations for their optimal PV:ELE ratio.

Table 4
Average yearly hydrogen production over the 20-year lifespan of each site/configuration for their optimal PV:ELE ratio.

Average yearly H_2 production (ton)			
	Tracker	Fixed	Δ%
Civitavecchia – Central Italy	51.83	44.77	15.7 %
Hamburg – Northern Germany	40.77	34.80	17.1 %
Zuara – Northern Libya	61.65	50.92	21.0 %

Table 5
Average yearly energy production over the 20-year lifespan of each site/configuration for their optimal PV:ELE ratio.

Average yearly energy production (MWh)			
	Tracker	Fixed	Δ%
Civitavecchia – Central Italy	2125	1784	19.1 %
Hamburg – Northern Germany	1465	1264	15.9 %
Zuara – Northern Libya	2461	2029	21.3 %

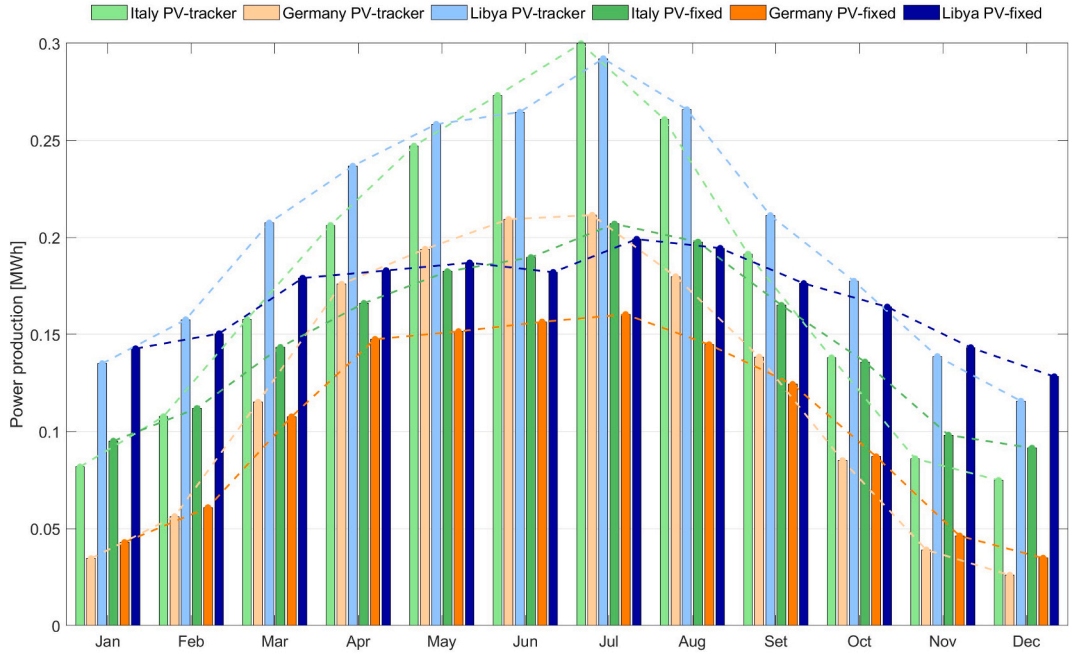


Fig. 5. Average monthly energy production over the 20-year lifespan for the three sites and two PV mounting configurations for their optimal PV:ELE ratio.

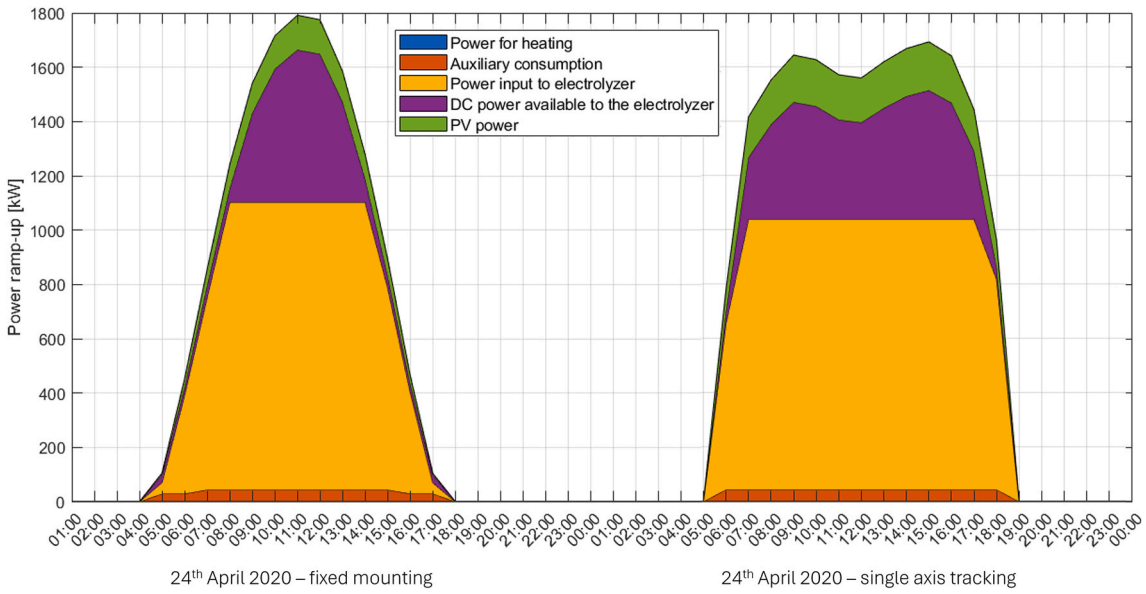


Fig. 6. Hourly power production and relative distribution between auxiliary, electrolyzer, curtailment and conversion loss on the pick production of year 2020 for Civitavecchia location fixed and tracker 1.6 MWp PV plant.

Table 6
Comparison between the PV and electrolyzer equivalent hours for each optimal ratio configuration.

	Average PV equivalent hours			Average ELE equivalent hours		
	Tracker	Fixed	Δ%	Tracker	Fixed	Δ%
Civitavecchia – Central Italy	2124	1783	19.13 %	2748	2287	20,16 %
Hamburg – Northern Germany	1464	1264	15.82 %	2162	1845	17,15 %
Zuara – Northern Libya	2461	2029	21.29 %	3269	2700	21,07 %

1) The **base strategy**, which emphasizes efficiency maximization through degradation-based prioritization of stack usage, achieves a consistent degradation profile across all stacks. As a result, replacement events are synchronized at the end of their useful life. This robust operational approach is illustrated in Fig. 7a.

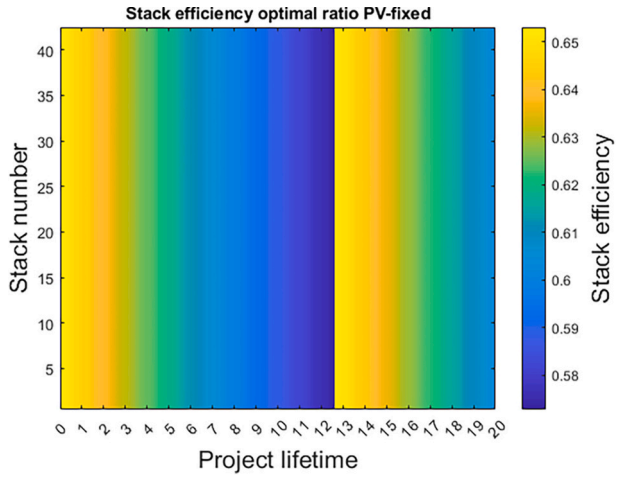


Fig. 7a. Example of stack efficiency map, base strategy, Civitavecchia – Tracking, ratio 1.5.

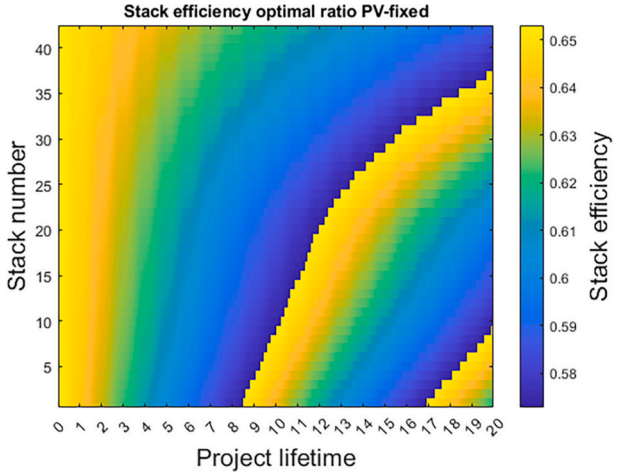


Fig. 7b. Example of stack efficiency map, non-optimized, Civitavecchia – Tracking, ratio 1.5.

2) In contrast, the **non-optimized strategy (Alternative 1),** leads to a heterogeneous degradation pattern due to its sequential utilization of stacks. This results in staggered replacements and potentially complicates long-term maintenance schedules, as illustrated in Fig. 7b.
3) The **mid-lifetime replacement strategy (Alternative 2)** introduces an early renewal cycle, replacing all stacks at year 10. When combined with a degradation-based prioritization usage strategy, it can lead to earlier replacements, ranging from 9 years.

   (Northern Germany – fixed systems) to 1 year (Northern Libya – tracker systems) earlier than the baseline strategy. This approach significantly enhances the efficiency of the hydrogen system during its second decade of operation, as illustrated in Fig. 7c.
4) Finally, **stack segregation (Alternative 3)** strategy operated based on stack degradation levels, with a variable number of stacks segregated and operated as a distinct set whenever the power saturation of the main set was reached. This approach aims to reduce the frequency of stack replacements by shifting the operational burden to fewer stacks, albeit at the expense of a slight reduction in overall system efficiency. An example of with is illustrated in Fig. 7d.

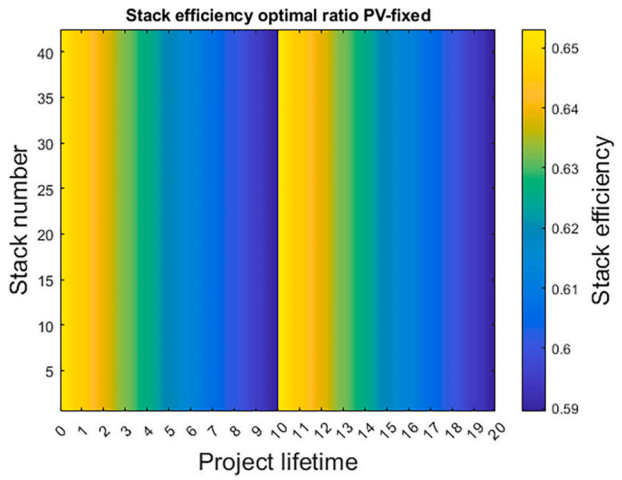


Fig. 7c. Example of stack efficiency map, mid-lifetime replacement strategy, Civitavecchia – Tracking, ratio 1.5.

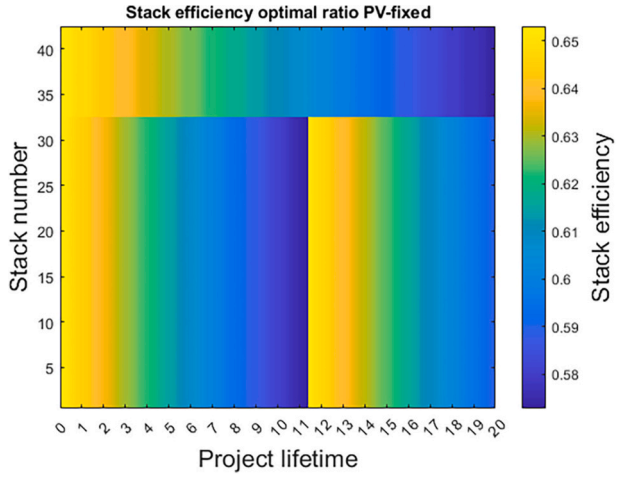


Fig. 7d. Example of stack efficiency map, stack segregation strategy, Civitavecchia – Tracking, ratio 1.5, 10 stack segregated.

Evaluating the LCOH associated with the four strategies analyzed, as well as the relative quantity of hydrogen produced, reveals minimal variations, generally within the range of 1–2 %. Regarding the mass of hydrogen produced under different strategies, when the ratio of photovoltaic nominal power to electrolyzer capacity is optimized as indicated in Table 3, the advantage of early stack replacement proposed in Alternative 2 diminishes by approximately 1 %, depending on the location and type of plant.

In the baseline scenario, the proposed algorithm for proper system sizing accounts for both the efficiency loss of the system and the behavior of irradiance curves, incorporating these factors into the determination of the optimal LCOH. As a result, while the increase in electrolyzer efficiency achieved through early stack replacement comes at the cost of earlier replacement expenses and reduced salvage revenue, it does not appear to provide significant benefits. Regarding Alternative Strategy 1, despite its already modest productivity advantages, the high frequency of stack replacement interventions required by this approach renders it impractical. At the same time, Alternative Strategy 3, while potentially reducing the number of stack replacements at the cost of a modest efficiency decrease, does not appear to offer significant advantages in reducing the LCOH. Moreover, it introduces an increased operational risk due to the prolonged 20-year use of a substantial portion of the stacks.

In conclusion, the optimal strategy for managing electrolyzer stacks coupled with photovoltaic production is the one proposed and modeled in Section 2.3. As a second best, the early stack replacement strategy, though slightly more expensive, can offer the potential advantage of balancing costs with operational efficiency by shortening the operational lifespan of the stacks and doing so potentially reducing the risk of near EOL failure.

When evaluating the operational risks associated with potential component failures, it is important to note that the modelled electrolyzer consists of 42 stacks, each further subdivided into 10 sub-units. As a result, maintenance interventions requiring the replacement of one or more sub-units are comparatively straightforward. Moreover, if one sub-unit within a stack malfunctions, only the affected stack is isolated for maintenance, allowing the rest of the facility to remain in operation. Although this approach decreases the total available power, it does not necessitate a complete shutdown. Consequently, the optimal strategy for stack management can evolve over time, taking into account any extraordinary maintenance activities or sub-unit replacements that may arise.

4. Conclusions

This work presents a techno-economic model that couples site-specific PV production with a stack-level electrolyser model incorporating thermal transients, start-up energy, degradation-driven efficiency decay and salvage value estimation. The aim is to identify the cost-optimal configurations by simulating, on an hourly basis over a 20-year period, the interchange between different PV production and electrolyzer operation to define the site-specific optimal PV:ELE ratio. By explicitly tracking the cumulative operating hours of each of the 42 AEM stacks and dynamically prioritising the least-degraded units, the model narrows the uncertainty of the LCOH estimations. Alternative operational strategies for stack utilization control are explored, and their techno-economic impacts are assessed in this study, additionally the cost-optimal configuration is investigated for two different mounting configurations, i.e., fixed and horizontal monoaxial sun tracker installation.

Applying the model to three climatically diverse sites shows that a horizontal mono-axial tracking array consistently outperforms a fixed-tilt installation, lowering the LCOH by about 10 % in Hamburg and 12 % in Zuara through a 15–21 % gain in annual hydrogen output. The cost-optimal PV:ELE nominal-power ratio is 1.6:1 in Zuara (northern Libya) and Civitavecchia (central Italy) and 1.8:1 in Hamburg (northern Germany). Departures of ±0.3 MW from these optima increase the LCOH by up to 4 %, with oversizing being more penalising at high-irradiance locations and undersizing at high latitudes. Under the best configuration the minimum LCOH reaches 4.47 €/kg in Zuara, whereas the highest value, 7.50 €/kg, is obtained for a fixed array in Hamburg. Ultimately, the analysis of alternative stack usage strategies highlights that balancing stack usage to maximise system efficiency at any given time is a reasonable approach that ensures LCOH is lower than any other tested alternatives.

Albeit this study offers more detailed modeling of both PV production and electrolyzer operation, accurately quantifying the residual value of electrolyzer stacks at the end of their service life remains challenging.

4.1. Future works

Several factors still limit the generalisability of these findings. First, stack ageing is assumed to be linear; long-term field data are required to calibrate more realistic degradation laws. Second, component prices, permitting charges and grid-connection fees are treated as location-independent, whereas regional cost heterogeneity could shift the optimum sizing. Third, the analysis is confined to a co-located of a MW scale plant; installations beyond the MW scale may benefit from economies of

scale but also face more complex integration constraints and exposure to transmission tariffs. Finally, market volatility for replacement parts and prospective technology improvements were not parameterised. Future work should therefore embed stochastic cost trajectories, include grid charges for non-co-located layouts and extend the model to larger systems to fully appraise the most cost-effective degree of production centralisation

CRediT authorship contribution statement

D. Vizza: Writing – original draft, Software, Methodology, Formal analysis, Conceptualization. **R. Caponi:** Writing – review & editing, Writing – original draft, Software, Methodology, Formal analysis, Conceptualization. **E. Bocci:** Supervision, Methodology, Investigation. **L. Del Zotto:** Visualization, Supervision. **C. Bassano:** Validation, Supervision, Data curation, Conceptualization.

Declaration of competing interest

The authors declare the following financial interests/personal relationships which may be considered as potential competing interests: Claudia Bassano reports financial support was provided by ENEA National Agency for New Technologies Energy and Economic Sustainable Development. Reports a relationship with that includes: If there are other authors, they declare that they have no known competing financial interests or personal relationships that could have appeared to influence the work reported in this paper.

Acknowledgment

This work was conducted under the '*Accordo di Programma MASE-ENEA sulla Ricerca di Sistema Elettrico – Piano Triennale di Realizzazione 2022–2024*' – Integrated project 'Hydrogen technologies', which is supported by the 'Fund for financing Research activities' established at 'Cassa per i servizi energetici e ambientali *(CSEA)*'.

Data availability

No data was used for the research described in the article.

References

[1] Kar SK, Harichandan S, Roy B. Bibliometric analysis of the research on hydrogen economy: an analysis of current findings and roadmap ahead. Int J Hydrogen Energy 2022;47(20):10803–24. https://doi.org/10.1016/j.ijhydene.2022.01.137.
[2] Fernández-Arias P, Antón-Sancho Á, Lampropoulos G, Vergara D. On green hydrogen generation technologies: a bibliometric review. Appl Sci 2024;14(6). https://doi.org/10.3390/app14062524.
[3] Genovese M, Schlüter A, Scionti E, Piraino F, Corigliano O, Fragiacomo P. Power-to-hydrogen and hydrogen-to-X energy systems for the industry of the future in Europe. Int J Hydrogen Energy 2023;48(44):16545–68. https://doi.org/10.1016/j.ijhydene.2023.01.194.
[4] Wei D, Li H, Ren Y, Yao X, Wang L, Jin K. Modeling of hydrogen production system for photovoltaic power generation and capacity optimization of energy storage system. Front Energy Res 2022;10. https://doi.org/10.3389/fenrg.2022.1004277.
[5] Wolf N, Kühn L, Höck M. International supply chains for a hydrogen ramp-up: techno-economic assessment of hydrogen transport routes to Germany. Energy Convers Manage: X 2024;23. https://doi.org/10.1016/j.ecmx.2024.100682.
[6] Reda B, Elzamar AA, AlFazzani S, Ezzat SM. Green hydrogen as a source of renewable energy: a step towards sustainability, an overview. In: Environment, development and sustainability. Springer Science and Business Media B.V; 2024. https://doi.org/10.1007/s10668-024-04892-z.
[7] Mazza A, Forte A, Bompard E, Cavina G, Angelini AM, Melani M. Assessment of the role of green hydrogen as the commodity enabling a new green dialogue among the Mediterranean shores. Energy Convers Manage: X 2024;23. https://doi.org/10.1016/j.ecmx.2024.100614.
[8] Guerra OJ, Eichman J, Kurtz J, Hodge BM. Cost competitiveness of electrolytic hydrogen. Joule 2019;3(10):2425–43. https://doi.org/10.1016/j.joule.2019.07.006.
[9] Hassan Q, Algburi S, Jaszczur M, Al-Jiboory AK, Al Musawi TJ, Ali BM, et al. Hydrogen role in energy transition: a comparative review. In: Process Safety and Environmental Protection. Institution of Chemical Engineers; 2024. p. 1069–93. https://doi.org/10.1016/j.psep.2024.02.030.
[10] Radner F, Strobl N, Köberl M, Rauh J, Esser K, Winkler F, et al. How to size regional electrolysis systems – simple guidelines for deploying grid-supporting electrolysis in regions with renewable energy generation. Energy Convers Manage: X 2023;20. https://doi.org/10.1016/j.ecmx.2023.100502.
[11] Yu B, Fang D, Xiao K, Pan Y. Drivers of renewable energy penetration and its role in power sector's deep decarbonization towards carbon peak. Renew Sustain Energy Rev 2023;178. https://doi.org/10.1016/j.rser.2023.113247.
[12] Crespi E, Colbertaldo P, Guandalini G, Campanari S. Energy storage with Power-to-Power systems relying on photovoltaic and hydrogen: modelling the operation with secondary reserve provision. J Storage Mater 2022;55:105613. https://doi.org/10.1016/j.est.2022.105613.
[13] Koleva M, Guerra OJ, Eichman J, Hodge BM, Kurtz J. Optimal design of solar-driven electrolytic hydrogen production systems within electricity markets. J Power Sources 2021;483. https://doi.org/10.1016/j.jpowsour.2020.229183.
[14] Glenk G, Reichelstein S. Economics of converting renewable power to hydrogen. Nat Energy 2019;4(3):216–22. https://doi.org/10.1038/s41560-019-0326-1.
[15] Andrews JW. Hydrogen production and carbon sequestration by steam methane reforming and fracking with carbon dioxide. Int J Hydrogen Energy 2020;45(16):9279–84. https://doi.org/10.1016/j.ijhydene.2020.01.231.
[16] Busse A, Power G, MacMurray J. Demonstration of carbon capture and sequestration of steam methane reforming process gas used for large-scale hydrogen production FINAL REPORT. PA (United States): Allentown; 2018.
[17] Ding JW, Fu YS, Lisa Hsieh IY. The cost of green: Analyzing the economic feasibility of hydrogen production from offshore wind power. Energy Convers Manage: X 2024;24. https://doi.org/10.1016/j.ecmx.2024.100770.
[18] Nasir M, Jordehi AR, Tostado-Véliz M, Tabar VS, Amir Mansouri S, Jurado F. Operation of energy hubs with storage systems, solar, wind and biomass units connected to demand response aggregators. Sustain Cities Soc 2022;83. https://doi.org/10.1016/j.scs.2022.103974.
[19] El Shamy AR, Aduama P, Al-Sumaiti AS. Chance constrained optimal sizing of a hybrid PV/battery/hydrogen isolated microgrid: a life-cycle analysis. Energ Conver Manage 2025;332. https://doi.org/10.1016/j.enconman.2025.119707.
[20] González del Valle A, García-Linares P, Martí A. Optimizing hydrogen production: a comparative study of direct and indirect coupling between photovoltaics and electrolyzer. Energ Conver Manage 2024;315. https://doi.org/10.1016/j.enconman.2024.118751.
[21] Cozzolino R, Bella G. A review of electrolyzer-based systems providing grid ancillary services: current status, market, challenges and future directions. In: Frontiers in Energy Research. Frontiers Media SA; 2024. https://doi.org/10.3389/fenrg.2024.1358333.
[22] Nguyen T, Abdin Z, Holm T, Mérida W. Grid-connected hydrogen production via large-scale water electrolysis. Energ Conver Manage 2019;200. https://doi.org/10.1016/j.enconman.2019.112108.
[23] Bukar AL, Chaitusaney S, Kawabe K. Optimal design of on-site PV-based battery grid-tied green hydrogen production system. Energ Conver Manage 2024;307. https://doi.org/10.1016/j.enconman.2024.118378.
[24] Coppitters D, De Paepe W, Contino F. Robust design optimization and stochastic performance analysis of a grid-connected photovoltaic system with battery storage and hydrogen storage. Energy 2020;213. https://doi.org/10.1016/j.energy.2020.118798.
[25] Dispenza G, Sergi F, Napoli G, Antonucci V, Andaloro L. Evaluation of hydrogen production cost in different real case studies. J Storage Mater 2019;24. https://doi.org/10.1016/j.est.2019.100757.
[26] Yang Y, De La Torre B, Stewart K, Lair L, Phan NL, Das R, et al. The scheduling of alkaline water electrolysis for hydrogen production using hybrid energy sources. Energ Conver Manage 2022;257. https://doi.org/10.1016/j.enconman.2022.115408.
[27] Dermühl S, Riedel U. A comparison of the most promising low-carbon hydrogen production technologies. Fuel 2023;340. https://doi.org/10.1016/j.fuel.2023.127478.
[28] Yukesh Kannah R, Kavitha S, Preethi, Parthiba Karthikeyan O, Kumar G, Dai-Viet NV, Rajesh Banu J. Techno-economic assessment of various hydrogen production methods – a review. Bioresour Technol 2021;319. https://doi.org/10.1016/j.biortech.2020.124175.
[29] Bhandari R, Adhikari N. A comprehensive review on the role of hydrogen in renewable energy systems. Int J Hydrogen Energy 2024;82:923–51. https://doi.org/10.1016/j.ijhydene.2024.08.004.
[30] Tashie-Lewis BC, Nnabuife SG. Hydrogen production, distribution, storage and power conversion in a hydrogen economy – a technology review. Chem Eng J Adv 2021;8. https://doi.org/10.1016/j.ceja.2021.100172.
[31] Roach M, Meeus L. The welfare and price effects of sector coupling with power-to-gas. Energy Econ 2020;86. https://doi.org/10.1016/j.eneco.2020.104708.
[32] Glenk G, Holler P, Reichelstein S. Advances in power-to-gas technologies: cost and conversion efficiency. Energ Environ Sci 2023;16(12):6058–70. https://doi.org/10.1039/d3ee01208e.
[33] Marzi E, Morini M, Saletti C, Vouros S, Zaccaria V, Kyprianidis K, et al. Power-to-Gas for energy system flexibility under uncertainty in demand, production and price. Energy 2023;284. https://doi.org/10.1016/j.energy.2023.129212.
[34] Blanco H, Faaij A. A review at the role of storage in energy systems with a focus on Power to Gas and long-term storage. Renew Sustain Energy Rev 2018;81:1049–86. https://doi.org/10.1016/j.rser.2017.07.062.
[35] Caponi R, Bocci E, Del Zotto L. On-site hydrogen refuelling station techno-economic model for a fleet of fuel cell buses. Int J Hydrogen Energy 2024;71:691–700. https://doi.org/10.1016/j.ijhydene.2024.05.216.

[36] Li Y, Liu F, Chen K, Liu Y. Technical and economic analysis of a hybrid PV/wind energy system for hydrogen refueling stations. Energy 2024;303. https://doi.org/10.1016/j.energy.2024.131899.
[37] IEA. *Global Hydrogen Review 2024*; 2024.
[38] Hydrogen Europe. *Clean Energy Monitor*; 2024.
[39] Guillotin A, Bergaentzlé C, Dussartre V, Heggarty T, Massol O, Perez Y. Hydrogen subsidies under three pillar-frameworks: a Europe-United States multi-stakeholder comparison. Renew Sustain Energy Rev 2025;211. https://doi.org/10.1016/j.rser.2024.115284.
[40] Yates J, Daiyan R, Patterson R, Egan R, Amal R, Ho-Baille A, et al. Techno-economic analysis of hydrogen electrolysis from off-grid stand-alone photovoltaics incorporating uncertainty analysis. Cell Rep Phys Sci 2020;1(10). https://doi.org/10.1016/j.xcrp.2020.100209.
[41] Sayedin F, Maroufmashat A, Sattari S, Elkamel A, Fowler M. Optimization of photovoltaic electrolyzer hybrid systems; taking into account the effect of climate conditions. Energ Conver Manage 2016;118:438–49. https://doi.org/10.1016/j.enconman.2016.04.021.
[42] Marocco P, Gandiglio M, Cianella R, Capra M, Santarelli M. Design of hydrogen production systems powered by solar and wind energy: an insight into the optimal size ratios. Energ Conver Manage 2024;314. https://doi.org/10.1016/j.enconman.2024.118646.
[43] Hassan Q, Abbas MK, Tabar VS, Tohidi S, Abdulrahman IS, Salman HM. Sizing electrolyzer capacity in conjunction with an off-grid photovoltaic system for the highest hydrogen production. Energy Harvest Syst 2023;10(2):331–48. https://doi.org/10.1515/ehs-2022-0107.
[44] Yang G, Zhang H, Wang W, Liu B, Lyu C, Yang D. Capacity optimization and economic analysis of PV–hydrogen hybrid systems with physical solar power curve modeling. Energ Conver Manage 2023;288. https://doi.org/10.1016/j.enconman.2023.117128.
[45] Grüger F, Dylewski L, Robinius M, Stolten D. Carsharing with fuel cell vehicles: Sizing hydrogen refueling stations based on refueling behavior. Appl Energy 2018;228:1540–9. https://doi.org/10.1016/j.apenergy.2018.07.014.
[46] Jamshidi M, Askarzadeh A. Techno-economic analysis and size optimization of an off-grid hybrid photovoltaic, fuel cell and diesel generator system. Sustain Cities Soc 2019;44:310–20. https://doi.org/10.1016/j.scs.2018.10.021.
[47] Gallardo F, García J, Monforti Ferrario A, Comodi G, Chiu JN. Assessing sizing optimality of OFF-GRID AC-linked solar PV-PEM systems for hydrogen production. Int J Hydrogen Energy 2022;47(64):27303–25. https://doi.org/10.1016/j.ijhydene.2022.06.098.
[48] Minutillo M, Perna A, Forcina A, Di Micco S, Jannelli E. Analyzing the levelized cost of hydrogen in refueling stations with on-site hydrogen production via water electrolysis in the Italian scenario. Int J Hydrogen Energy 2021;46(26):13667–77. https://doi.org/10.1016/j.ijhydene.2020.11.110.
[49] Kim M, Lee D, Qi M, Kim J. Techno-economic analysis of anion exchange membrane electrolysis process for green hydrogen production under uncertainty. Energ Conver Manage 2024;302. https://doi.org/10.1016/j.enconman.2024.118134.
[50] Chen PH, Chen WS, Lee CH, Wu JY. Comprehensive review of crystalline silicon solar panel recycling: from historical context to advanced techniques. Sustainability 2024;16(1). https://doi.org/10.3390/su16010060.
[51] Du N, Roy C, Peach R, Turnbull M, Thiele S, Bock C. Anion-exchange membrane water electrolyzers. in chemical reviews (Vol. 122, Issue 13, pp. 11830–11895). American Chemical Society; 2022. doi: 10.1021/acs.chemrev.1c00854.
[52] OECD. *Reaching Climate Neutrality for the Hamburg Economy by 2040*. Paris; 2024. https://doi.org/10.1787/e1e44672-en.
[53] Regione Lazio. *Piano di Transizione Ecologica di Civitavecchia 2022-2026*; 2022.
[54] Van Hoecke L, Laffineur L, Campe R, Perreault P, Verbruggen SW, Lenaerts S. Challenges in the use of hydrogen for maritime applications. Energ Environ Sci 2021;14(2):815–43. https://doi.org/10.1039/d0ee01545h.
[55] Ouki M. *Italy and its North African gas interconnections: A potential Mediterranean gas "hub"?*; 2023.Retrieved from https://sonatrach.com/wp-.